RESEARCH ARTICLE | DECEMBER 01 2023

Ultrafast photoinduced carrier transfer dynamics in monolayer MoS₂/graphene heterostructure *⊙*

Ben Liu; Lihe Yan **№** (; Jinhai Si (); Yanan Shen; Xun Hou



J. Appl. Phys. 134, 213101 (2023) https://doi.org/10.1063/5.0174742





Articles You May Be Interested In

A self-powered solar-blind photodetector based on polyaniline/ α -Ga $_2$ O $_3$ p–n heterojunction

Appl. Phys. Lett. (October 2021)

Probing the charge and heat transfer channels in optically excited graphene — transition metal dichalcogenide hybrids using Johnson noise thermometry

Appl. Phys. Lett. (July 2022)

Compositional engineering of interfacial charge transfer in van der Waals heterostructures of graphene and transition metal dichalcogenides

J. Chem. Phys. (August 2024)





Ultrafast photoinduced carrier transfer dynamics in monolayer MoS₂/graphene heterostructure

Cite as: J. Appl. Phys. 134, 213101 (2023); doi: 10.1063/5.0174742 Submitted: 2 September 2023 · Accepted: 6 November 2023 · Published Online: 1 December 2023







Ben Liu, Lihe Yan,a) D Jinhai Si, D Yanan Shen, and Xun Hou

AFFILIATIONS

Key Laboratory for Physical Electronics and Devices of the Ministry of Education and Shaanxi Key Lab of Photonic Technique for information, School of Electronics Science and Engineering, Faculty of Electronic and Information Engineering, Xi'an Jiaotong University, Xi'an 710049, China

a) Author to whom correspondence should be addressed: liheyan@mail.xjtu.edu.cn

ABSTRACT

Two-dimensional molybdenum disulfide (MoS₂) has been proved to be a good candidate in photodetectors, and MoS₂/graphene (MoS₂/G) heterostructure has been widely used to expand the optical response to two-color pump-probe measurements are performed. By comparing the carrier dynamics in MoS₂ and MoS₂/G under different pump wavelengths, we find that interfacial excitons are formed in the heterostructure, and fast hot carriers transfer (<200 fs) from graphene to MoS₂ are observed. The results indicate that the formed heterostructure with graphene can not only expand the optical response wavelength of MoS₂ but also improve the response time of the device in the near-infrared region.

Published under an exclusive license by AIP Publishing. https://doi.org/10.1063/5.0174742 heterostructure has been widely used to expand the optical response wavelength of MoS2. To clarify the carrier transfer dynamics in the

I. INTRODUCTION

Photodetectors have been widely applied in various fields, including optical sensing, imaging, optical communications, etc.1-Compared with traditional semiconductors, two-dimensional (2D) materials exhibit outstanding advantages such as atomic thickness, adjustable bandgap, high photoelectric responsivity, and well flexibility, meeting the needs of future photodetectors with higher performance and smaller size.5-7 In recent years, 2D molybdenum disulfide (MoS2) has become a research focus in the field of photodetectors, benefiting from its unique properties of flexible preparation, layer dependent physical properties, and adjustable photoelectrical response.^{8–10} For example, Radisavljevic *et al.* in 2011 prepared a field effect transistor based on high-quality monolayer MoS_2 with a mobility of $\sim 200 \text{ cm}^2 \text{ V}^{-1} \text{ S}^{-1}$ at room temperature, which is comparable to that achieved in silicon thin films. 11 Yin et al. fabricated a novel phototransistor based on mechanically exfoliated monolayer MoS2 nanosheets for the first time, which showed better photoresponsivity than graphenebased devices. 12 Based on the temperature-dependent photoconductivity of MoS₂, Di Bartolomeo et al. reported recently that the photoconductivity of MoS₂ transistors increases with increasing temperature, above room temperature under ambient pressure.

However, due to the limitation of the intrinsic bandgap of MoS₂, its spectral responsivity is often limited to the visible light range.14-16

To adjust the absorption spectral range, different methods including electric field regulation, chemical doping, and constructing heterostructures with other 2D materials have been proposed to control the bandgap of 2D MoS₂ materials. Among these methods, the MoS₂/graphene (MoS₂/G) heterostructure proved to be an effective strategy to improve the performance of MoS2-based photodetectors due to the unique properties of graphene with extremely high carrier mobility, very low resistivity, 17 and zerobandgap. 18 Studies of the past few years have demonstrated that graphene can form junctions with 2D semiconducting materials that showed rectifying characteristics and behaved as excellent Schottky diodes. 19 In recent years, many studies have achieved higher responsivity and wider operating wavelength by introducing graphene into MoS2-based photodetectors. For example, Vabbina et al. fabricated a MoS2/G photodetector with a maximum photo responsivity of 1.26 AW-1 and a wide range of wavelengths from visible region to mid-infrared region.² Xu et al. prepared a graphene-MoS2 hybrid phototransistor with a high responsivity of 10 AW⁻¹, which is much higher than that

of an individual graphene phototransistor or a MoS₂-based phototransistor.²¹ The heterostructure can not only expand the absorption spectrum of the material but also modulate the photophysical response dynamics because of the charge transfer between different 2D materials. There are some studies about the interlayer charge transfer in 2D heterostructures, and a femtosecond pump-probe transient absorption technique is commonly used to study these processes. For example, Xu et al. have studied the interlayer transfer dynamics in MoS₂/G heterostructures by ultrafast spectroscopy.²² However, there is an initial rapid transfer of electrons from graphene to the MoS₂ layer, which cannot be well resolved due to the relatively lower temporal resolution of the system. Recently, Zou et al. observed the formation and relaxation of interfacial excitons in MoS₂/G heterostructures and proposed that the hot electrons in graphene are transferred to MoS₂ within 0.5 ps.²³ However, direct evidence of hot electron transfer from graphene to MoS2 has not been demonstrated, and the charge transfer as well as the relaxation processes of interlayer carriers in MoS2/G heterostructures still need further study.

In this work, we studied the carrier dynamics of monolayer MoS₂ and MoS₂/G heterostructure using femtosecond transient absorption (TA) and time-resolved two-color pump-probe spectroscopy. We studied the transfer process of interlayer carriers under different energy pump lights. Our experimental results show that when the pump light energy is lower than the bandgap of MoS₂, the electrons in graphene are transferred to MoS2, and the time of this process is shorter than 200 fs; when the pump light energy is higher than the MoS₂ bandgap, the holes in MoS₂ are transferred to graphene, which takes about 800 fs.

II. MATERIALS AND METHODS

A. Synthesis of MoS₂/G heterostructures

The monolayer MoS₂ films on sapphire substrates were prepared using the chemical vapor deposition (CVD) method. The MoS₂/G heterostructures were prepared in the following two steps: the monolayer graphene film was first grown on a copper foil via the CVD process and then, transferred onto the top of the monolayer MoS₂ film grown on a 1.0 mm-thick sapphire substrate.

B. Instruments and measurements

UV-vis absorption spectra of the samples were obtained from a spectrophotometer (UV-2600, China). Raman spectra were acquired from a Raman system (HR800, France) with 532 nm laser excitation. X-ray photoelectron spectroscopy (XPS) experiments were carried out with an x-ray photoelectron spectrometer (ESCALAB Xi⁺, USA).

TA spectra of the samples were measured using a home-built femtosecond time-resolved TA setup.^{24,25} A mode-locked Ti:sapphire amplifier system (Vitesse, Conherent) was used (central wavelength: 800 nm, pulse duration: 50 fs, repetition rate: 1 kHz) as the laser source. The output was split into two beams: the stronger one of which was frequency doubled to generate a 400 nm pump light and the other one was focused into a sapphire plate to generate a broadband supercontinuum probe light (ranging from 450 to 750 nm). Using an optical chopper, the repetition rate of the pump pulse was adjusted to 500 Hz and was focused on the sample with probe light. TA spectra were obtained by comparing the probe light spectra with and without pump light excitation. By adjusting the delay time between pump and probe pulses, TA spectra changes as a function of the delay time were recorded. The TA spectra were acquired at room temperature and ambient pressure.

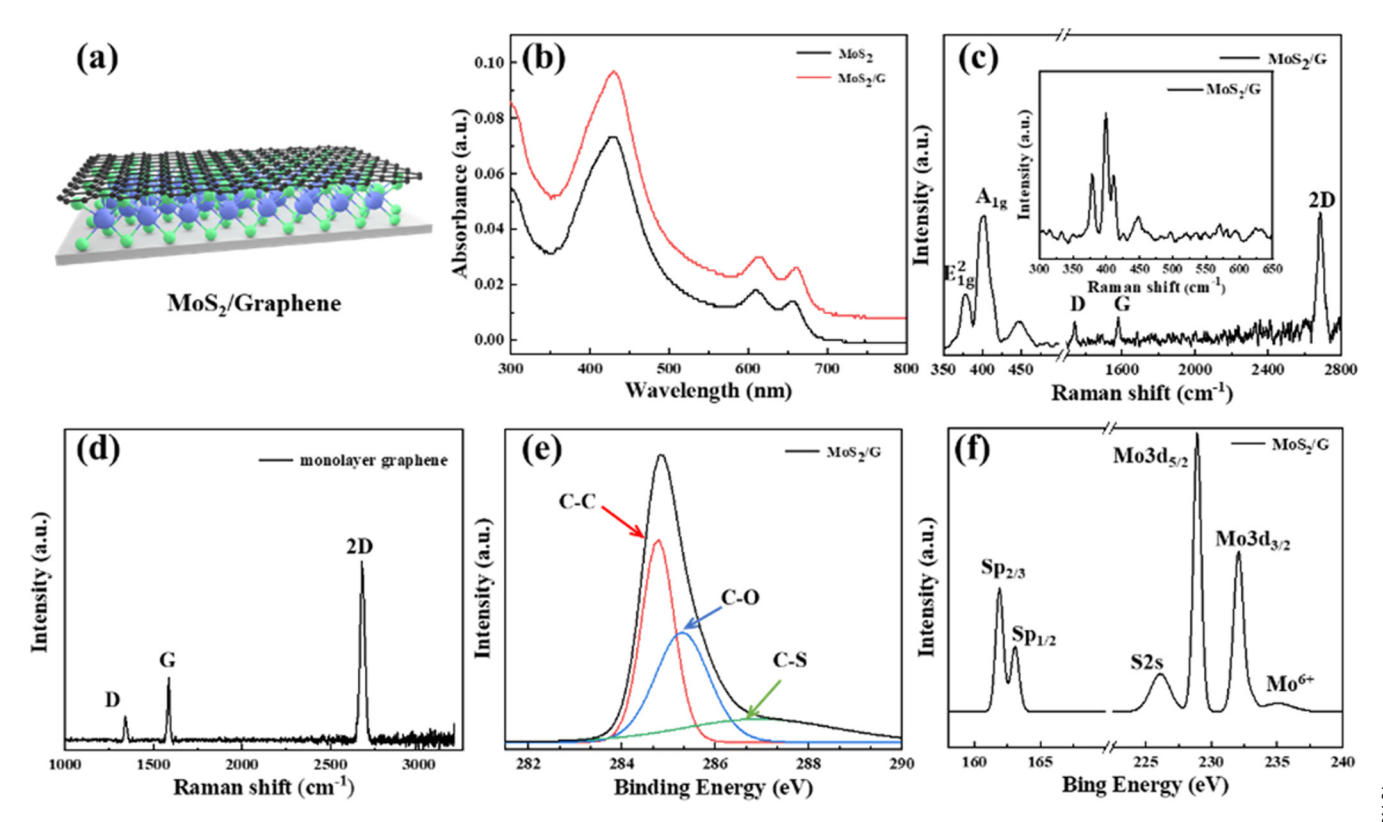
Time-resolved two-color pump-probe spectroscopy was performed under ambient conditions at room temperature. The system used the femtosecond laser mentioned above and an optical parametric amplifier (OPA) as the laser source. In the measurements, an 800 nm fundamental laser and a frequency-doubled 400 nm laser were used as the pump light, respectively, and the output with different wavelengths from the OPA was used as the probe light. The pump and probe pulses were focused into the sample simultaneously, and the pump-probe time delay was controlled using a motorized translation stage. The time-resolved transmission signal was measured by a photodetector and a lock-in amplifier.

III. RESULT AND DISCUSSION

A. Characterization of materials

The schematic structure of the MoS₂/G heterostructure is shown in Fig. 1(a). The absorption signals of MoS₂/G and MoS₂ are shown in Fig. 1(b). The spectra reveal strong absorption at 480 nm, and two weak peaks at around 620 and 670 nm in MoS₂, representing the absorption of A (670 nm), B (620 nm), and C (480 nm) excitons, ^{26–28} respectively. Furthermore, intensity of the absorption peak of the graphene/MoS2 heterojunction is stronger than that of pure MoS₂. We attribute this to the wide absorption range of graphene from ultraviolet to terahertz.²

Two characteristic peaks in the Raman spectrum of MoS₂/G are observed in Fig. 1(c). The inset of Fig. 1(c) shows the magnified view of 300–650 cm⁻¹ given in Fig. 1(c). Two main peaks located at $\frac{80}{90}$ 380.4 and 401.1 cm⁻¹ are attributed to the A_{1g} and E_{2g} vibration modes in MoS₂. The E_{2g} mode can be attributed to the in-plain $\frac{1}{2}$ vibration of the Mo-S bonds in MoS2, and the A1g mode corresponds to the out-of-plane vibration of S atoms in MoS₂. The difference between the E_{2g} peak and the A_{1g} peak (20.7 cm⁻¹) is less than 21 cm⁻¹, indicating that the MoS₂ film is monolayer. ^{31,32} The peaks located at around 1350, 1560, and 2750 cm⁻¹ correspond to the D, G, and 2D peaks of graphene in the MoS₂/G heterostructure, respectively. The intensity ratio between the 2D and G bands is about 2, which is consistent with the Raman spectroscopy results of graphene in Fig. 2(d), indicating that graphene is single-layer with high quality.³³ The chemical composition and elements of MoS₂/G heterostructures are further determined using XPS. The C spectrum of MoS₂/G shows three peaks [Fig. 2(e)], located near 284.8, 285.3, and 287.3 eV, belonging to the C-C, C-O, and C-S bonds, respectively.³⁴ These C-peaks demonstrate a strong interaction coupling between MoS2 and graphene in the heterojunction structures.30 Figure 2(f) shows the S2p and Mo3d spectra of MoS_2/G . The $2p_{3/2}$ peak at 161.9 and $2p_{1/2}$ peak at 163.1 eV are attributed to the -2 valence state of the S atom and the S peak at 226 eV is ascribed to S2s in MoS_2 . The high-resolution XPS spectra of Mo show three peaks at 228.9, 232, and 235 eV, corresponding to Mo3d_{5/2}, Mod_{3/2}, and Mo⁶⁺ of MoS₂, respectively.³⁶ Furthermore, the existence of Mo⁶⁺ demonstrates that the Mo edge in MoS₂ is oxidized during the preparation process.



h spectra of MoS₂ and MoS₂/G films. (c) Raman spectra of MoS₂ (blue) and –650 cm⁻¹ region of MoS₂/G heterostructure Raman spectra. (d) Raman spectra of XPS spectra of S2p and Mo3d in MoS₂/G.

bandgap of MoS₂, no signal can be observed in the pure MoS₂ film [as shown by the inset of Fig. 2(c)]. As graphene can be excited by 800 pm limit in the pure MoS₂ film and the spectra of Fig. 2(c)]. FIG. 1. (a) Schematics of the MoS2/G heterostructure. (b) Steady-state absorption spectra of MoS2 and MoS2/G films. (c) Raman spectra of MoS2 (blue) and MoS₇/G (black) heterostructures. The inset of (c) shows the magnified view of the 300-650 cm⁻¹ region of MoS₂/G heterostructure Raman spectra. (d) Raman spectra of monolayer graphene. (e) XPS spectra of C element in the MoS₂/G heterostructure. (f) XPS spectra of S2p and Mo3d in MoS₂/G.

B. TA spectra of MoS₂ and MoS₂/G

The charge transfer dynamics in the monolayer MoS₂ film and the MoS₂/G heterostructure were studied using femtosecond time-resolved TA spectroscopy. The typical time-resolved TA spectra of the monolayer MoS₂ film under 400 nm excitation are shown in Fig. 2(a). The TA spectra show five characteristic signal peaks. The two dips at 660 and 610 nm correspond to the decrease of A and B exciton absorption [as shown by the UV-vis spectra given in Fig. 1(b)], respectively.³⁷ When the probe light irradiates MoS₂ films, electrons in the valence band absorb the incident photons to form electron-hole pairs of bound states (A and B excitons). In the pump-probe measurement, the electrons in the exciton are excited to the conduction band after pump light irradiation, causing bleaching of the exciton states and two dips at 660 and 610 nm in the TA spectra. The three positive peaks are located at 670, 640, and 480 nm, which may be attributed to peak shift and broadening of A/B/C exciton states, respectively.³⁸ The spectra of MoS₂/G heterostructures under 400 nm excitation are shown in Fig. 2(b), which shows the same characteristic TA peaks as monolayer MoS₂. To confirm the charge transfer between the MoS₂ and graphene layers in the heterostructure, we selected 800 nm wavelength pump pulses to excite pure MoS₂ film and MoS₂/G heterojunction, respectively. As the excitation energy is lower than the

800 nm light, significant TA signals can be observed in the MoS₂/G heterojunction [as shown in Fig. 2(c)], indicating that the excited carrier is able to be transferred from graphene to MoS2. Figure 2(d) displays the decay process of the absorption change of MoS₂/G at 480 nm under different excitation wavelengths. However, the signal-to-noise ratio of the curve under 800 nm excitation is too low to compare the detailed decay processes under different excitation conditions.

C. Charge transfer between MoS₂ and graphene

In order to further study the transfer of excited carriers, a time-resolved two-color pump-probe spectroscopy with higher sensitivity is used for measurements. Here, a 480 nm laser from the OPA is used as the probe, and the fundamental 800 nm and frequency-doubled 400 nm light are used as the pump light, respectively. The 400 nm (3.1 eV) pump pulse is used to excite both MoS₂ and graphene, while the 800 nm (1.55 eV) pump pulse is used to excite only graphene in the heterostructure.

Figure 3(a) shows the decay process of carrier dynamics in monolayer MoS2 and MoS2/G heterostructure. The pump and probe wavelengths were 400 and 480 nm, respectively. The decay

10 November 2025 06:09:42

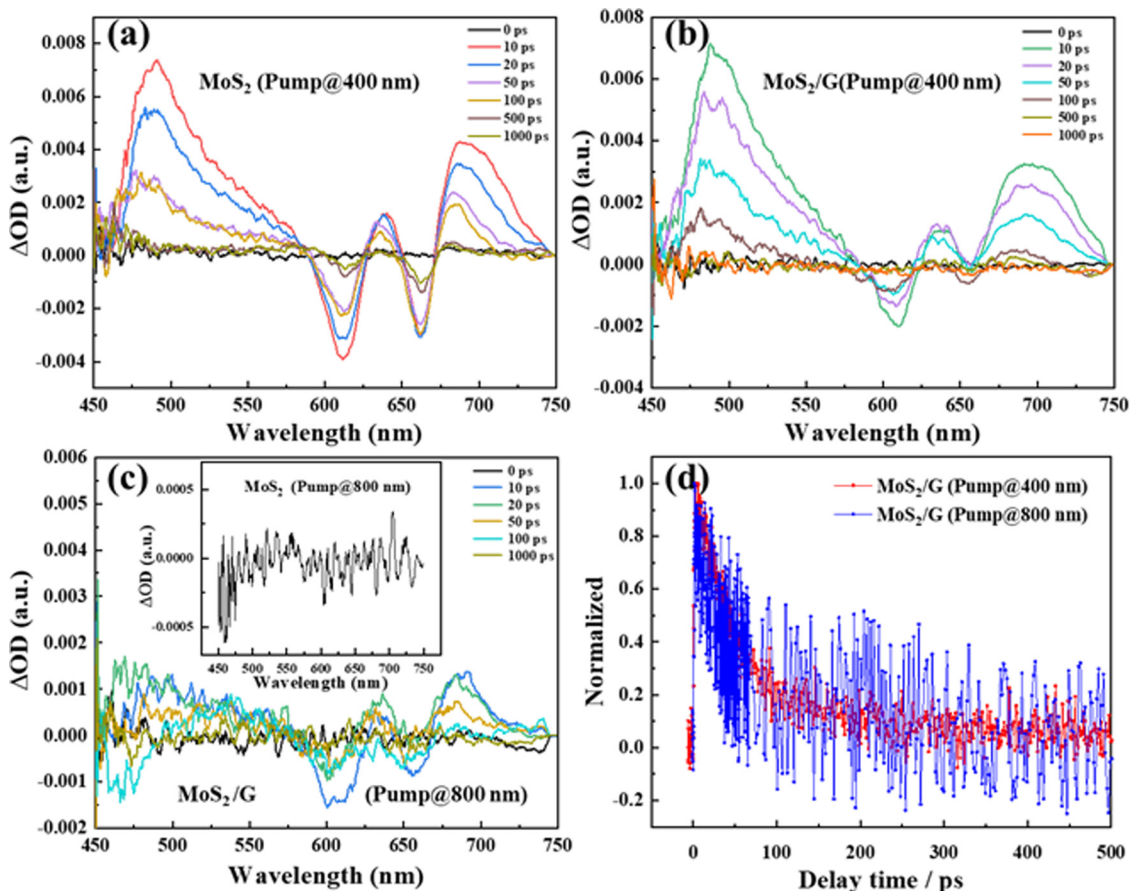


FIG. 2. (a) Femtosecond TA spectra of monolayer MoS_2 with 400 nm excitation. (b) Femtosecond TA spectra of the MoS_2/G heterostructure with 400 nm excitation. (c) Femtosecond TA spectra of the MoS_2/G heterostructure with 800 nm excitation. The inset of (c) shows the femtosecond TA spectra of monolayer MoS_2 with 800 nm excitation. (d) Comparison of carrier dynamics of MoS_2/G under different excitation wavelengths.

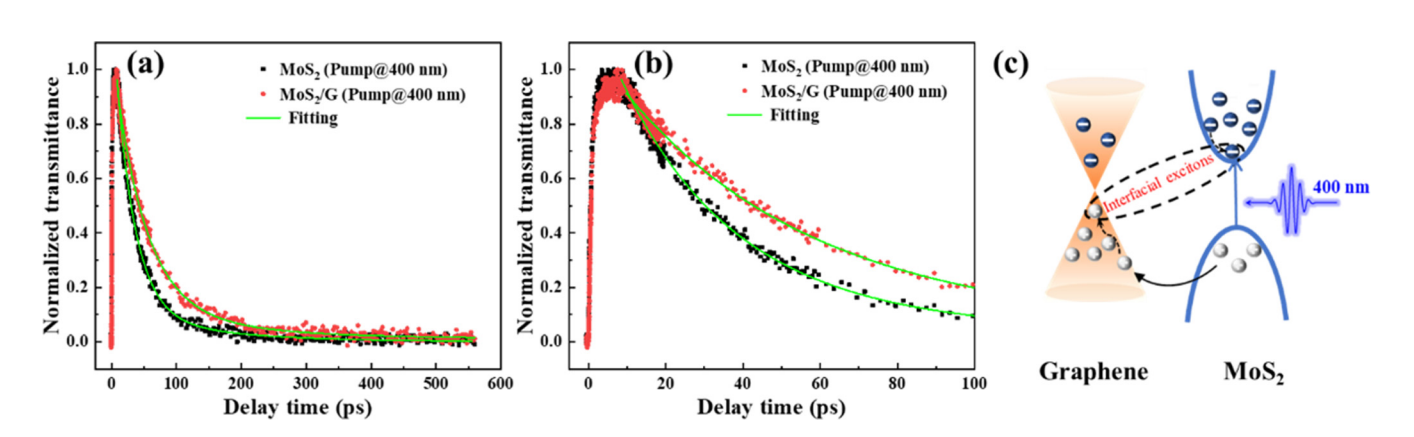


FIG. 3. Normalized time-resolved TR experiment results of monolayer MoS_2 (black squares) and MoS_2/G (red circles) heterostructures under 400 nm excitation. (b) Zoomed-in area of (a) for the first 100 ps delay time. (c) Illustration of hot holes in MoS_2 transferred to graphene after excitation at 400 nm and forming interfacial excitons with electrons in the MoS_2 conduction band.

TABLE I. Fitting results for the two-color pump-probe experiment under different excitation wavelengths.

	Arising time (ps)	Delay time (ps)	
Sample	$ au_{ m arising}$	$\tau_{ m decay1}$	$\tau_{ m decay2}$
MoS ₂ (pump at 400 nm)	_	29 (88%)	135 (12%)
MoS ₂ /G (pump at 400 nm)	0.8	47 (87%)	169 (13%)
MoS ₂ /G (pump at 800 nm)	0.2	6 (36%)	107 (64%)

signals of MoS2 and MoS2/G are well-fitted using a multi-exponential decay function (green curves). There are two carrier relaxation processes in MoS2. The fast relaxation time (29 ps) with an amplitude of ~88% could be attributed to intraband carrier-carrier interactions and the slow relaxation time (135 ps) with an amplitude of ~12% corresponds to interband carrier-phonon interactions.³⁹ Notably, the lifetime of the MoS₂/G heterostructure was markedly longer than that of the monolayer MoS2 film.

There are also two carrier relaxation processes in the MoS₂/G heterostructure. Corresponding fitting parameters are summarized in Table I. The fast relaxation time (47 ps) with an amplitude of ~87% is attributed to the hole relaxation of graphene and intraband carrier-carrier interactions of MoS2. The slow relaxation time (169 ps) with an amplitude of ~13% is obviously longer than that in pure MoS₂. We believe that the slow relaxation process in MoS₂/G heterojunctions includes not only the carrier-phonon interactions within MoS₂ but also the relaxation process occurring in the interface excitons between MoS2 and graphene. Since the photon energy of the pump pulse is above the bandgap of MoS₂, both MoS₂ and graphene in MoS₂/G can be excited. The pump light injects electron-hole pairs into MoS2 and graphene. The photogenerated holes on the top valence band of MoS2 can transfer to the valance band of graphene. 23,40 Therefore, the holes remaining in the conduction band of MoS2 and the electrons in the valence band of graphene form interfacial excitons. By analyzing the relaxation time of carriers in the MoS₂ and MoS₂/G heterojunctions mentioned above, the carrier dynamics in the MoS₂/G heterojunction under 400 nm excitation are plotted in the schematic diagram shown in Fig. 3(c).

We further study the carrier transfer process in the MoS₂/G heterostructure upon 800 nm excitation. As the excitation energy is below the bandgap of MoS₂, the pump injects electron-hole pairs directly into graphene only. We still observed the relaxation signal of MoS₂ exciton at 480 nm probe, as shown in Fig. 4(a) (blue triangles). This indicates that the MoS₂/G heterostructure also responds in the near-infrared band and has a wider absorption range than the monolayer MoS2. In this case, we consider that the hot electrons are rapidly transferred from the conduction band of graphene to the conduction band of MoS₂, and interfacial excitons are formed with holes in the valence band of graphene, as shown in Fig. 4(c).

There are two carrier relaxation processes in MoS₂/G under 800 nm excitation. The fast relaxation time (6 ps) with an amplitude of over 36% is attributed to the relaxation process of hot electrons in the conduction band of graphene and MoS₂. The slow relaxation time (107 ps) with an amplitude of ~64% is mainly due to the relaxation process of interfacial excitons, and trap states induced recombination at the interface of graphene and MoS2 could also contribute. The aforementioned MoS2/G heterostructure carrier dynamics process under 400 nm excitation is shown in Fig. 4(a) (red circles). We compare the rising time of the two signals, as shown in Fig. 4(b). We found that the of the two signals, arriving time of the heterostructure signal under 800 nm exemulation (~200 fs) is significantly shorter than that under 400 nm excitation (~800 fs). Because of the high carrier mobility shorter than that under 400 nm excitation (~800 fs). Because of the high carrier mobility and narrow bandgap of graphene, we believe that the fast-rising time in the MoS₂/G heterostructure under 800 nm excitation is attributed to the hot electron transfer from the graphene conduction band to the MoS2 conduction § band. Therefore, the formed heterostructure with graphene can $\frac{\Theta}{k}$ not only expand the optical response wavelength of the MoS₂-based photodetectors but also improve the response time of the device in the near-infrared region.

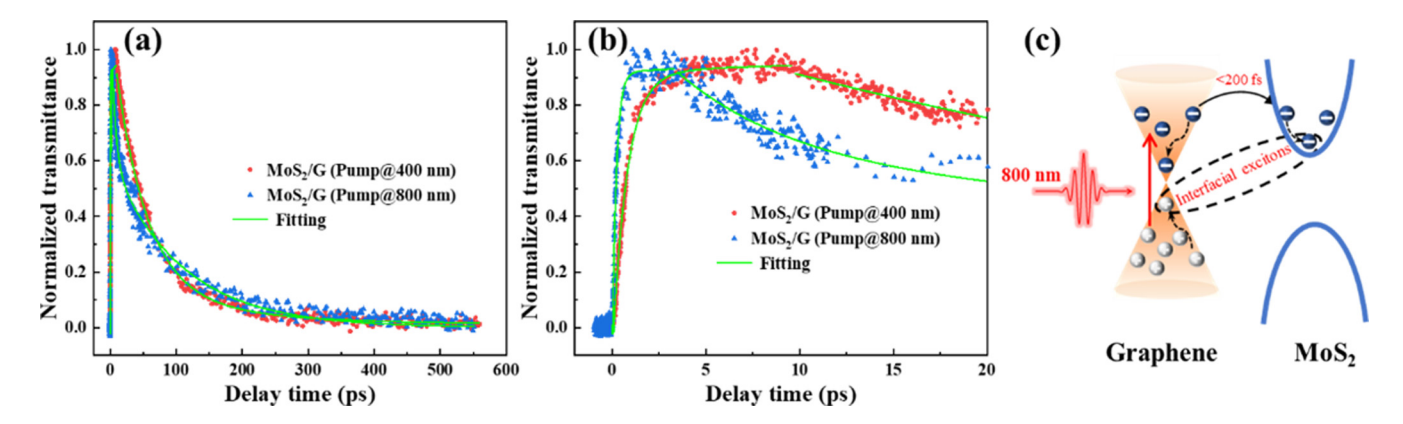


FIG. 4. Normalized time-resolved TR experiment result of the monolayer MoS₂/G heterostructure under 400 (red circles) and 800 nm (blue triangles). (b) Zoomed-in area of (a) for the first 20 ps delay time. (c) Illustration of hot electrons in graphene transferred to MoS₂ after excitation at 800 nm and forming interfacial excitons with holes in the graphene valence band.

IV. CONCLUSION

In summary, we have investigated the charge transfer dynamics in MoS₂/G heterostructures using femtosecond time-resolved TA and time-resolved two-color pump-probe spectroscopy techniques. We studied the response time and mechanism of carrier transfer by adjusting the excitation wavelength. Upon excitation above the MoS₂ bandgap, hot holes in MoS₂ are transferred to graphene, resulting in the formation of interfacial excitations with electrons in MoS2. The ultrafast hole transfer time and the formation time of interfacial excitons is about 800 fs. When the pump energy is below the bandgap of MoS2, hot electrons in graphene are transferred to MoS₂, resulting in the formation of interfacial excitations with electrons in MoS2 and holes in graphene. The measured ultrafast electron transfer time is shorter than 200 fs, which could improve the response time of MoS2-based photodetectors. This work is helpful to understand the ultrafast dynamic of photogenerated carriers in the MoS₂/G heterostructure, which is very important for the application of MoS2-based heterostructures in high-performance optoelectronic devices such as broadband, high-response, and highspeed photodetectors.

ACKNOWLEDGMENTS

This work was supported by the National Natural Science Foundation of China (NNSFC) (Grant No. 62027822) and the National R&D Program of China (Grant No. 2019YFA0706402).

AUTHOR DECLARATIONS

Conflict of Interest

The authors have no conflicts to disclose.

Author Contributions

Ben Liu: Data curation (lead); Formal analysis (lead); Investigation (lead); Methodology (lead); Writing - original draft (lead); Writing - review & editing (lead). Lihe Yan: Methodology (equal); Resources (equal); Writing - review & editing (equal). Jinhai Si: Funding acquisition (supporting); Resources (supporting); Supervision (supporting). Yanan Shen: Investigation (equal). Xun Hou: Resources (supporting); Supervision (supporting).

DATA AVAILABILITY

The data that support the findings of this study are available from the corresponding author upon reasonable request.

REFERENCES

- ¹X. Li, M. Zhu, M. Du, Z. Lv, L. Zhang, Y. Li, Y. Yang, T. Yang, X. Li, K. Wang, H. Zhu, and Y. Fang, "High detectivity graphene-silicon heterojunction photodetector," Small 12(5), 595-601 (2016).
- ²C. Bao, J. Yang, S. Bai, W. Xu, Z. Yan, Q. Xu, J. Liu, W. Zhang, and F. Gao, "High performance and stable all-inorganic metal halide perovskite-based photodetectors for optical communication applications," Adv. Mater. 30(38), 1803422
- ³X. Hu, X. Zhang, L. Liang, J. Bao, S. Li, W. Yang, and Y. Xie, "High-performance flexible broadband photodetector based on organolead halide perovskite," Adv. Funct. Mater. 24(46), 7373-7380 (2014).

- ⁴N. Huo and G. Konstantatos, "Recent progress and future prospects of 2D-based photodetectors," Adv. Mater. 30(51), 1801164 (2018).
- ⁵D. H. Kang, M. S. Kim, J. Shim, J. Jeon, H. Y. Park, W. S. Jung, H. Y. Yu, C. H. Pang, S. Lee, and J. H. Park, "High-performance transition metal dichalcogenide photodetectors enhanced by self-assembled monolayer doping," Adv. Funct. Mater. 25(27), 4219-4227 (2015).
- ⁶H. Xu, A. Ren, J. Wu, and Z. Wang, "Recent advances in 2D MXenes for photodetection," Adv. Funct. Mater. 30(24), 2000907 (2020).
- ⁷Q. Qiu and Z. Huang, "Photodetectors of 2D materials from ultraviolet to terahertz waves," Adv. Mater. 33(15), 2008126 (2021).
- 8H. S. Lee, S.-W. Min, Y.-G. Chang, M. K. Park, T. Nam, H. Kim, J. H. Kim, S. Ryu, and S. Im, "MoS2 nanosheet phototransistors with thickness-modulated optical energy gap," Nano Lett. 12(7), 3695-3700 (2012).
- ⁹Y.-Y. Lai, Y.-W. Yeh, A.-J. Tzou, Y.-Y. Chen, Y. S. Wu, Y.-J. Cheng, and H.-C. Kuo, "Dependence of photoresponsivity and on/off ratio on quantum dot density in quantum dot sensitized MoS₂ photodetector," Nanomaterials **10**(9), 1828 (2020). ¹⁰Z. Li, J. Wu, C. Wang, H. Zhang, W. Yu, Y. Lu, and X. Liu, "High-performance
- monolayer MoS2 photodetector enabled by oxide stress liner using scalable chemical vapor growth method," Nanophotonics 9(7), 1981-1991 (2020).
- 11 B. Radisavljevic, A. Radenovic, J. Brivio, V. Giacometti, and A. Kis, "Single-layer MoS₂ transistors," Nat. Nanotechnol. 6(3), 147-150 (2011).
- 12 Z. Yin, H. Li, H. Li, L. Jiang, Y. Shi, Y. Sun, G. Lu, Q. Zhang, X. Chen, and H. Zhang, "Single-layer MoS₂ phototransistors," ACS Nano 6(1), 74-80 (2012).
- ¹³A. Di Bartolomeo, A. Kumar, O. Durante, A. Sessa, E. Faella, L. Viscardi, K. Intonti, F. Giubileo, N. Martucciello, P. Romano, S. Sleziona, and M. Schleberger, "Temperature-dependent photoconductivity in two-dimensional MoS₂ transistors," Mater. Today Nano 24, 100382 (2023).
- ¹⁴O. Lopez-Sanchez, D. Lembke, M. Kayci, A. Radenovic, and A. Kis, "Ultrasensitive photodetectors based on monolayer MoS2," Nat. Nanotechnol. 8(7), 497-501 (2013).
- 15 S. Manzeli, D. Ovchinnikov, D. Pasquier, O. V. Yazyev, and A. Kis, "2D transition metal dichalcogenides" Nat. Rev. Mater. 2(8), 1–15 (2017). tion metal dichalcogenides," Nat. Rev. Mater. 2(8), 1-15 (2017).
- 16W. Tang, C. Liu, L. Wang, X. Chen, M. Luo, W. Guo, S.-W. Wang, and W. Lu, "MoS₂ nanosheet photodetectors with ultrafast response," Appl. Phys. Lett.
- 111(15), 153502 (2017).

 17 J. Chen, J. Xi, D. Wang, and Z. Shuai, "Carrier mobility in graphyne should be even larger than that in graphene: A theoretical prediction," J. Phys. Chem. Lett. 4(9), 1443–1448 (2013).
- ¹⁸B. Y. Zhang, T. Liu, B. Meng, X. Li, G. Liang, X. Hu, and Q. J. Wang, "Broadband high photoresponse from pure monolayer graphene photodetector," Nat. Commun. 4(1), 1811 (2013).
- 19 A. Di Bartolomeo, "Graphene Schottky diodes: An experimental review of the rectifying graphene/semiconductor heterojunction," Phys. Rep. 606, 1-58 (2016). ²⁰P. Vabbina, N. Choudhary, A.-A. Chowdhury, R. Sinha, M. Karabiyik, S. Das, W. Choi, and N. Pala, "Highly sensitive wide bandwidth photodetector based on internal photoemission in CVD grown p-type MoS₂/graphene Schottky junction," ACS Appl. Mater. Interfaces 7(28), 15206-15213 (2015).
- 21 H. Xu, J. Wu, Q. Feng, N. Mao, C. Wang, and J. Zhang, "High responsivity and gate tunable graphene-MoS₂ hybrid phototransistor," Small 10(11), 2300-2306
- ²²Z. Xu, Z. Liu, D. Zhang, Z. Zhong, and T. B. Norris, "Ultrafast dynamics of charge transfer in CVD grown MoS2-graphene heterostructure," Appl. Phys. Lett. 119(9), 093102 (2021).
- 23Y. Zou, Q.-S. Ma, Z. Zhang, R. Pu, W. Zhang, P. Suo, K. Sun, J. Chen, D. Li, H. Ma, X. Lin, Y. Leng, W. Liu, J. Du, and G. Ma, "Observation of ultrafast interfacial exciton formation and relaxation in graphene/MoS2 heterostructure," J. Phys. Chem. Lett. 13(23), 5123-5130 (2022).
- ²⁴T. Huo, L. Yan, J. Si, P. Ma, and X. Hou, "Ultrafast photoinduced carrier dynamics in single crystalline perovskite films," J. Mater. Chem. C 11(11), 3736-3742 (2023).
- ²⁵C. Wang, L. Yan, J. Si, T. Huo, and X. Hou, "Strongly luminescent and highly stable CsPbBr3/Cs4PbBr6 core/shell nanocrystals and their ultrafast carrier dynamics," J. Alloys Compd. 946, 169272 (2023).

- ²⁶K. Wang, J. Wang, J. Fan, M. Lotya, A. O'Neill, D. Fox, Y. Feng, X. Zhang, B. Jiang, Q. Zhao, H. Zhang, J. N. Coleman, L. Zhang, and W. J. Blau, "Ultrafast saturable absorption of two-dimensional MoS₂ nanosheets," ACS Nano 7(10), 9260–9267 (2013).
- ²⁷H. Shi, R. Yan, S. Bertolazzi, J. Brivio, B. Gao, A. Kis, D. Jena, H. G. Xing, and L. Huang, "Exciton dynamics in suspended monolayer and few-layer MoS₂ 2D crystals," ACS Nano 7(2), 1072–1080 (2013).
- ²⁸S. H. Aleithan, M. Y. Livshits, S. Khadka, J. J. Rack, M. E. Kordesch, and E. Stinaff, "Broadband femtosecond transient absorption spectroscopy for a CVD MoS₂ monolayer," Phys. Rev. B 94(3), 035445 (2016).
- ²⁹Y. Xu, L. Yan, J. Si, M. Li, Y. Ma, J. Li, and X. Hou, "Nonlinear absorption properties and carrier dynamics in MoS₂/graphene van der Waals heterostructures," Carbon 165, 421–427 (2020).
- ³⁰X. Sun, B. Zhang, Y. Li, X. Luo, G. Li, Y. Chen, C. Zhang, and J. He, "Tunable ultrafast nonlinear optical properties of graphene/MoS₂ van der Waals heterostructures and their application in solid-state bulk lasers," ACS Nano 12(11), 11376–11385 (2018).
- ³¹Y. Xie, Z. Wang, Y. Zhan, P. Zhang, R. Wu, T. Jiang, S. Wu, H. Wang, Y. Zhao, T. Nan, and X. Ma, "Controllable growth of monolayer MoS₂ by chemical vapor deposition via close MoO₂ precursor for electrical and optical applications," Nanotechnology 28(8), 084001 (2017).
- ³²S. Kataria, S. Wagner, T. Cusati, A. Fortunelli, G. Iannaccone, H. Pandey, G. Fiori, and M. C. Lemme, "Growth-induced strain in chemical vapor deposited monolayer MoS₂: Experimental and theoretical investigation," Adv. Mater. Interfaces 4(17), 1700031 (2017).
- 33 R. Liu, B. Liao, X. Guo, D. Hu, H. Hu, L. Du, H. Yu, G. Zhang, X. Yang, and Q. Dai, "Study of graphene plasmons in graphene-MoS₂ heterostructures for optoelectronic integrated devices," Nanoscale 9(1), 208–215 (2017).
- optoelectronic integrated devices," Nanoscale 9(1), 208–215 (2017).

 34P. Zhao, M. Ni, Y. Xu, C. Wang, C. Chen, X. Zhang, C. Li, Y. Xie, and J. Fei,

 "A novel ultrasensitive electrochemical quercetin sensor based on MoS₂-carbon nanotube @ graphene oxide nanoribbons/HS-cyclodextrin/graphene quantum dots composite film," Sens. Actuators B 299, 126997 (2019).
- 35J. Shi, M. Liu, J. Wen, X. Ren, X. Zhou, Q. Ji, D. Ma, Y. Zhang, C. Jin, H. Chen, S. Deng, N. Xu, Z. Liu, and Y. Zhang, "All chemical vapor deposition

- synthesis and intrinsic bandgap observation of MoS₂/graphene heterostructures," Adv. Mater. 27(44), 7086–7092 (2015).
- 36Y. Xu, L. Yan, X. Li, and H. Xu, "Fabrication of transition metal dichalcogenides quantum dots based on femtosecond laser ablation," Sci. Rep. 9(1), 2931 (2019).
- ³⁷Y. Li, J. Shi, H. Chen, Y. Mi, W. Du, X. Sui, C. Jiang, W. Liu, H. Xu, and X. Liu, "Slow cooling of high-energy C excitons is limited by intervalley-transfer in monolayer MoS₂," Laser Photonics Rev. **13**(4), 1800270 (2019).
- ³⁸L. Wang, Z. Wang, H.-Y. Wang, G. Grinblat, Y.-L. Huang, D. Wang, X.-H. Ye, X.-B. Li, Q. Bao, A.-S. Wee, S. A. Maier, Q.-D. Chen, M.-L. Zhong, C.-W. Qiu, and H.-B. Sun, "Slow cooling and efficient extraction of C-exciton hot carriers in MoS₂ monolayer," Nat. Commun. 8(1), 13906 (2017).
- ³⁹Z. Nie, R. Long, L. Sun, C.-C. Huang, J. Zhang, Q. Xiong, D. W. Hewak, Z. Shen, O. V. Prezhdo, and Z.-H. Loh, "Ultrafast carrier thermalization and cooling dynamics in few-layer MoS₂," ACS Nano 8(10), 10931–10940 (2014).
- ⁴⁰S. Fu, I. du Fossé, X. Jia, J. Xu, X. Yu, H. Zhang, W. Zheng, S. Krasel, Z. Chen, Z. M. Wang, K.-J. Tielrooij, M. Bonn, A. J. Houtepen, and H. I. Wang, "Long-lived charge separation following pump-wavelength-dependent ultrafast charge transfer in graphene/WS₂ heterostructures," Sci. Adv. 7(9), eabd 9061 (2021).
- $^{\bf 41}$ W. Zhang, J. K. Huang, C. H. Chen, Y. H. Chang, Y. J. Cheng, and L. J. Li, "High-gain phototransistors based on a CVD MoS $_2$ monolayer," Adv. Mater. **25**(25), 3456–3461 (2013).
- ⁴²S. H. Mir, V. K. Yadav, and J. K. Singh, "Recent advances in the carrier mobility of two-dimensional materials: A theoretical perspective," ACS Omega 5(24), 14203–14211 (2020).
- ⁴³C. M. Orofeo, H. Hibino, K. Kawahara, Y. Ogawa, M. Tsuji, K.-i. Ikeda, S. Mizuno, and H. Ago, "Influence of Cu metal on the domain structure and carrier mobility in single-layer graphene," Carbon 50(6), 2189–2196 (2012).
- ⁴⁴S. Zhang, M. Xie, F. Li, Z. Yan, Y. Li, E. Kan, W. Liu, Z. Chen, and H. Zeng, "Semiconducting group 15 monolayers: A broad range of band gaps and high carrier mobilities," Angew. Chem. Int. Ed. 55(5), 1666–1669 (2016).